JATIS Journal of Astronomical Telescopes, Instruments, and Systems

RESEARCH PAPER

Non-ionizing radiation effects in a soft X-ray CMOS image sensor

Charles Townsend-Rose,* Thomas W. Buggey, James M. Ivory, Imane Dazzazi, Konstantin D. Stefanov, and David J. Hall
The Open University, Centre for Electronic Imaging, Milton Keynes, United Kingdom

ABSTRACT. CIS221-X is a prototype monolithic complementary metal-oxide-semiconductor (CMOS) image sensor, optimized for soft X-ray astronomy and developed for the proposed European Space Agency Transient High Energy Sky and Early Universe Surveyor (THESEUS) mission. One significant advantage of CMOS technology is its resistance to radiation damage. To assess this resistance, three backside-illuminated CIS221-X detectors have been irradiated with 10 MeV protons using the MC40 Cyclotron Facility at the University of Birmingham, United Kingdom. Each detector received 1/2, 1, and 2 THESEUS end-of-life proton fluences (6.65×10^8 p^+/cm^2). One had already been exposed to ionizing radiation [up to 59.04 krad total ionizing dose (TID)] during a previous radiation campaign. Using unirradiated readout electronics, the electro-optical performance of each device has been measured before and after proton irradiation. No significant change was observed in the readout noise and image lag. An increase in mean dark current was recorded, as was an increase in the number of hot pixels. The degradation of CIS221-X performance due to non-ionizing radiation effects is similar to that of comparable CMOS image sensors and has been attributed to an increase in the number of bulk silicon defects.

 [DOI: 10.1117/1.JATIS.10.3.036002]

Keywords: CMOS image sensor; soft X-ray astronomy; X-ray detectors; radiation damage; total non-ionizing dose.

Paper 24115G received Jul. 20, 2024; revised Sep. 3, 2024; accepted Sep. 5, 2024; published Sep. 24, 2024.

1 Introduction

The Transient High Energy Sky and Early Universe Surveyor (THESEUS)[1–3] is a proposed European Space Agency (ESA) Cosmic Vision M7 mission to monitor the whole sky for high-energy transients, particularly gamma-ray bursts. To achieve the science objectives of the mission, the THESEUS spacecraft design includes three science instruments:

- Soft X-ray Imager (SXI, 0.3 to 5 keV), a set of two soft X-ray monitors using micropore optics (MPO) and complementary metal-oxide-semiconductor (CMOS) image sensors;
- X/Gamma-rays Imaging Spectrometer (XGIS, 2 keV to 10 MeV), a set of two X/gamma-ray monitors using coded-aperture masks and SSDs coupled to CsI crystal scintillators;
- InfraRed Telescope (0.7 to 1.8 μm), a Korsch telescope using HgCdTe detectors.

THESEUS is designed for a low inclination (5.4 deg) low Earth orbit, with a nominal altitude between 550 and 640 km. This orbit minimizes exposure to charged particles trapped in the Earth's van Allen belts, providing a low and stable background for the XGIS instrument.

*Address all correspondence to Charles Townsend-Rose, charles.townsend-rose@open.ac.uk

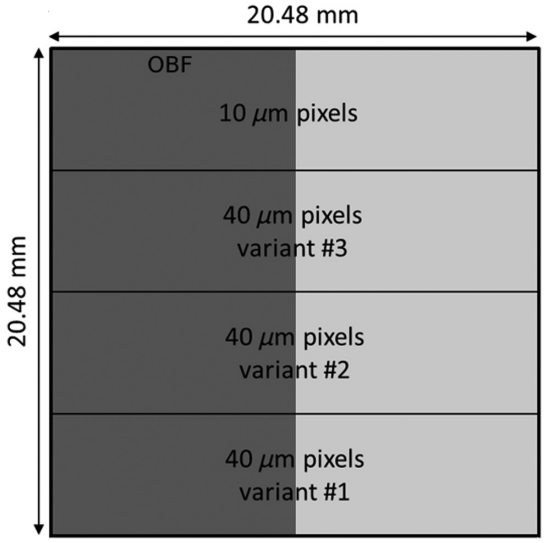

Fig. 1 Diagram of the CIS221-X image area.

It also offers near-complete shielding from solar particle events and galactic cosmic rays. However, the orbit does feature periodic transits through the South Atlantic Anomaly, during which the spacecraft will be exposed to high levels of radiation.

The THESEUS SXI end-of-life (EoL) radiation dose has been determined through comprehensive modeling, using an approach that considers both the unfocused radiation that passes through the spacecraft and the focused radiation that is directed by the MPO.[4] At the end of the nominal three-year mission, the SXI CMOS image sensors are predicted to receive 0.18 krad total ionizing dose (TID) and a proton fluence of 6.65×10^8 $p^+(10\ \text{MeV})/\text{cm}^2$.

A prototype soft X-ray CMOS image sensor, named CIS221-X,[5] has been developed for the THESEUS SXI instrument. The sensor features 35 μm thick, high-resistivity epitaxial silicon, which can be over-depleted by reverse substrate bias due to the inclusion of deep depletion extension implants[6] in the 4T pinned photodiode pixel design. As illustrated in Fig. 1, the CIS221-X image area comprises four equally sized regions: three 40 μm pitch square pixel variants and one region of 10 μm pitch square pixels. All three of the 40 μm pixel variants feature an additional pinning implant to help mitigate the increase in image lag due to the large pixel size. Furthermore, the additional pinning implant of the 40 μm "variant #2" pixels has a novel "Christmas tree" shape, and the "variant #3" pixels have a larger transfer gate. Some CIS221-X devices feature an optical blocking filter (OBF) covering half of each pixel region.

A comprehensive electro-optical characterization of the CIS221-X[7] showed that, with the exception of dark current, the sensor meets or outperforms the beginning-of-life requirements for the THESEUS mission. To assess how this performance would degrade over the spacecraft's lifetime, radiation damage tests have been completed. A study of ionizing radiation effects showed degradation similar to that of comparable CMOS image sensors.[8] More recently, non-ionizing radiation effects have been measured.[9]

For the study of non-ionizing radiation effects, the European Space Components Coordination advocates the use of a particle accelerator to provide a flux of high-energy protons.[10] These protons interact elastically with a target material, releasing atoms from the lattice, causing displacement damage. This can degrade a CMOS image sensor's performance, resulting in an increase in dark current and a rise in the number of defective pixels.[11,12] Using the MC40 cyclotron facility at the University of Birmingham, United Kingdom, three backside-illuminated (BSI) CIS221-X devices have been irradiated with protons up to and beyond the THESEUS EoL total non-ionizing dose (TNID). The impact on electro-optical performance has been measured.

2 Methods

The MC40 cyclotron facility at the University of Birmingham, United Kingdom, can provide a beam of up to 1×10^{13} protons/s/cm^2 with a chosen energy 2.7 to 40 MeV.[15] In October 2023,

Table 1 BSI CIS221-X devices selected for proton irradiation and corresponding TID and TNID.

Serial no. 21094-	OBF/non-OBF	Proton fluence [p^+ (10 MeV)/cm^2]	TID[b] (krad)	TNID[c] (MeV/g)
03-16	Non-OBF	—	—	—
03-11[a]	Non-OBF	3.33×10^8	0.185	3.13×10^6
07-03	OBF	6.65×10^8	0.371	6.25×10^6
06-31	OBF	1.33×10^9	0.742	1.25×10^7

[a]Previously exposed to ionizing radiation up to 59.04 krad TID.[8]
[b]Calculated using ionizing energy loss data.[13]
[c]Calculated using non-ionizing energy loss data.[14]

three BSI CIS221-X image sensors were irradiated with 10 MeV protons at the MC40 cyclotron facility. Table 1 details the devices selected for testing, the received proton fluence, and the equivalent TID and TNID. One device acted as a control, whereas the other three were irradiated with proton fluences of 1/2, 1, and 2 THESEUS EoL (6.65×10^8 p^+/cm^2). To simplify testing and allow for comparison with the literature, irradiations were conducted at room temperature and pressure. It is recommended that once the final THESEUS SXI flight model sensors are manufactured, they be retested under representative in-orbit conditions. Each irradiation lasted ~1 min, during which the devices were unbiased with all pins grounded. One of the proton-irradiated devices (03-11) had previously been exposed to ionizing radiation up to 59.04 krad TID.[8] During the ~6 months between ionizing radiation testing and proton irradiation, this device was stored at room temperature.

The performance of each image sensor was measured using unirradiated readout electronics before and after proton irradiation. The post-irradiation device characterizations were conducted 1 to 14 days after the irradiation, and the sensors were stored at room temperature. Annealing may have occurred during this time, although further work is necessary to determine whether this has significantly impacted our results. Data collection was completed with the image sensors in a vacuum ($<10^{-5}$ hPa), operated over-depleted by reverse substrate bias (−20 V), and cooled to −40°C.

3 Results and Discussion

All CIS221-X 40 μm pixels degraded at similar rates following exposure to proton irradiation. As a previous electro-optical characterization has shown that optimal performance is found in the 40 μm "variant #3" pixels,[7] only the results from this variant are presented. To understand how the 40 μm pixel modifications have impacted the sensor's non-ionizing radiation hardness, results from the 10 μm pixels are also shown for comparison. Due to insufficient data, the post-irradiation gain of the 03-11 10 μm pixels could not be measured. Consequentially, only the pre-irradiation results are presented for these pixels. No measurable change was recorded for all parameters of the control device. Uncertainty values have been determined using either one standard deviation of the data distribution or, when the data has been fit to a Gaussian, one standard deviation of the parameter estimate. All results have corresponding uncertainties, although most are too small to be seen as error bars.

3.1 Conversion Gain

Using Mn X-ray fluorescence and with a 15 ms integration time, the CIS221-X conversion gain was measured before and after proton irradiation. As seen in Fig. 2, no measurable change was observed in the gain of all devices except 03-11, which increased.

One possible explanation for the increase in gain for the 03-11 device is that the high dark current in this sensor is influencing the gain measurement. 03-11 was previously irradiated up to 59.04 krad TID and showed an increase in dark current due to incurred ionizing radiation damage.[8] As will be shown in Sec. 3.3, before proton irradiation, the 03-11 dark current was higher than all other devices and, following proton irradiation, increased significantly. It has been

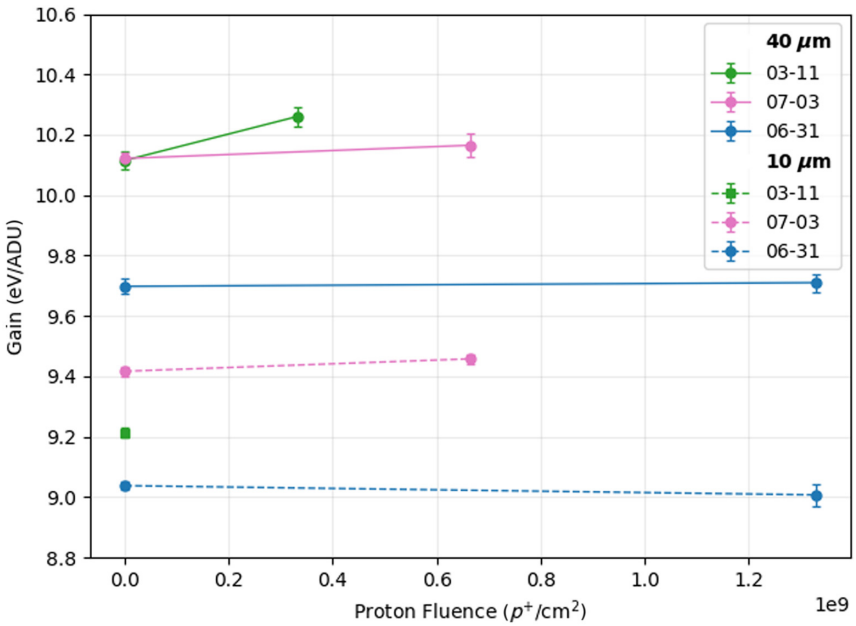

Fig. 2 CIS221-X conversion gain measured at increasing proton fluence.

reported that the CIS221-X non-linearity grows with increasing signal,[7] implying that the gain is also non-linear. Due to a greater pre-proton irradiation dark current, the 03-11 pre-irradiation gain was measured at a higher signal value than the other devices. Furthermore, due to the increase in dark current following proton irradiation, the 03-11 post-irradiation gain is measured at an even higher signal value. The non-linearity of the CIS221-X gain, the already high pre-irradiation dark current, and the significant increase post-irradiation would result in an increase in gain for the 03-11 device. This explanation could be validated by remeasuring the gain with different integration times and observing how the varying dark signal influences the measurement.

3.2 Readout Noise

The per-pixel readout noise was measured using 50 dark frames with a readout time of 0.2 s and the dark current suppressed (transfer gate voltage, $V_{TG} = 0$ V). Figure 3 shows that no significant change was observed in the readout noise of all devices following proton irradiation. The 03-11 readout noise is ~1.5 e^-RMS greater than the other CIS221-X devices due to damage incurred during previous ionizing radiation testing.[8]

3.3 Dark Current

As previously reported,[7] the CIS221-X dark current exhibits large-scale non-uniformity across the image area. To examine how the dark current changes following proton irradiation, a locally uniform 50×50 pixel region was selected for analysis. All data were collected with the image sensor cooled to −40°C.

Figure 4 shows the dark current increased in all devices following proton irradiation. The rate of degradation was greatest in the device previously exposed to ionizing radiation, 03-11. Although the dark current of the CIS221-X Non-OBF pixels is greater than that of the OBF pixels, the rate of increase with proton fluence is similar for each half of the image area. For the 10 μm pixels, the dark current increased ~×16 less than it did in the 40 μm pixels, corresponding to the difference in pixel area. The per-pixel dark current distribution of the 06-31 40 μm OBF pixels is shown in Fig. 5. Not only has the mean dark current increased following proton irradiation, but the tail of the histogram has lengthened. This behavior was exhibited by all pixels of all devices and suggests an increase in hot pixels following proton irradiation. The scale of degradation of CIS221-X dark current following proton irradiation is similar to that of comparable CMOS image sensors.[11,12]

The CIS221-X silicon bulk can be depleted by applying a reverse substrate bias V_{BSB}, with full depletion expected at −11 V.[16] Figure 6 shows the CIS221-X dark current measured for

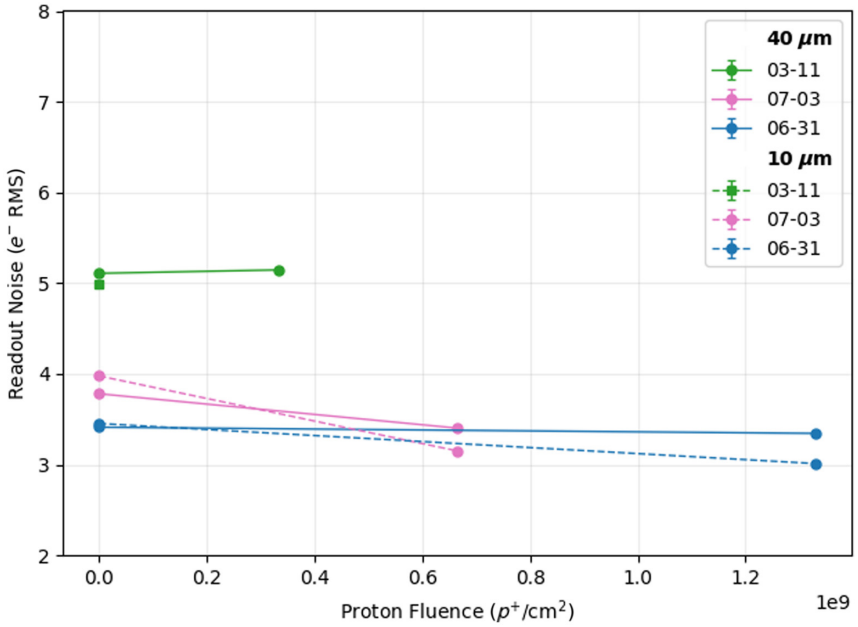

Fig. 3 CIS221-X readout noise measured at increasing proton fluence with dark current suppressed.

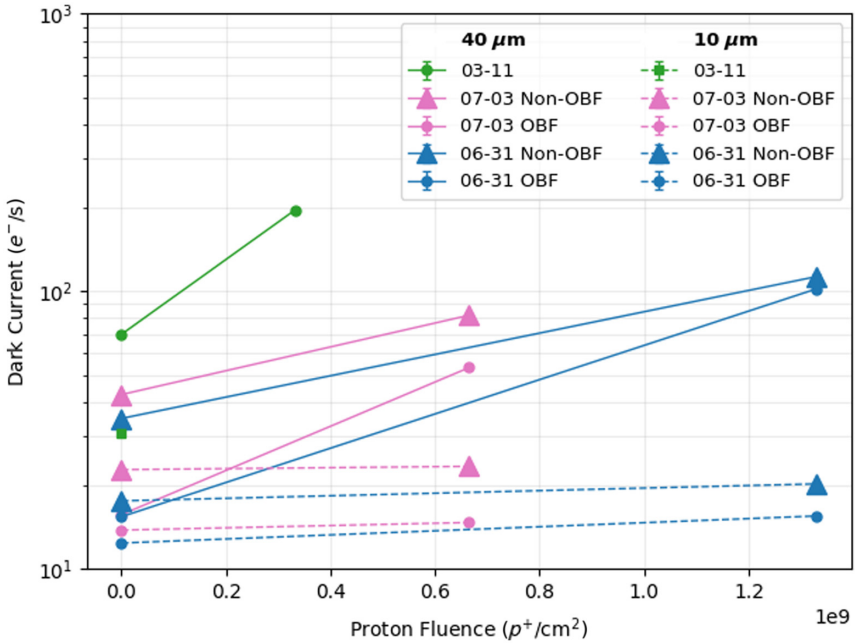

Fig. 4 CIS221-X dark current measured at increasing proton fluence with the image sensor cooled to −40°C.

different V_{BSB} voltages before and after proton irradiation. For all devices, the post-irradiation dark current increases with reverse bias as the depletion region extends out through the substrate and captures a greater number of damage sites. This confirms that the observed increase in dark current following proton irradiation is due to an increase in the number of bulk silicon defects. For the 07-03 and 06-31 devices, the dark current stabilizes at approximately −10 V, indicating full depletion. However, for the device previously exposed to ionizing radiation, 03-11, the dark current continues to increase for V_{BSB} beyond −10 V and does not stabilize within the range measured (≥ -25 V). This could suggest that the device is not reaching full depletion or there is an additional mechanism driving an increase in dark current. Further work is necessary to determine if either of these explanations is true or if the result is simply an outlier.

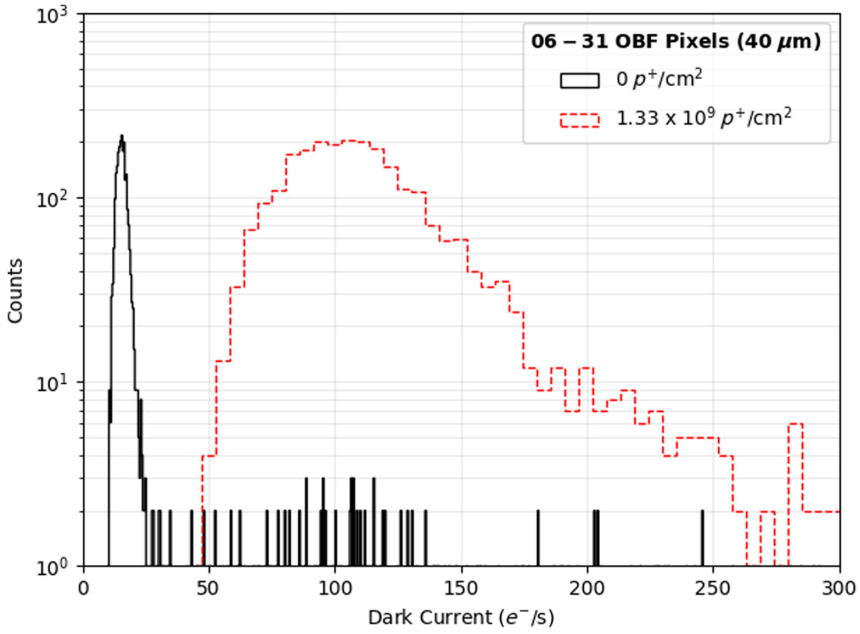

Fig. 5 Dark current distribution of 06-31 40 μm OBF pixels measured before and after proton irradiation with the image sensor cooled to −40°C.

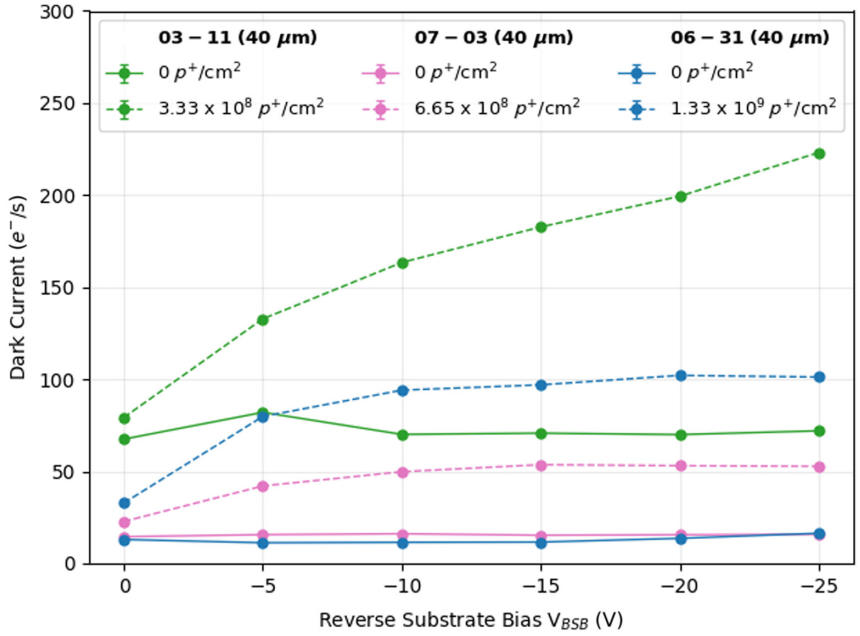

Fig. 6 CIS221-X dark current measured at increasing proton fluence with the image sensor cooled to −40°C and operated at different reverse substrate biases, V_{BSB}.

3.4 Image Lag

CIS221-X leading-edge image lag was measured using pulsed light-emitting diode (LED) illumination. The lag was only measurable in the non-OBF pixels because the OBF blocked all of the LED signal. Furthermore, as the 10 μm pixels collect ×16 less signal than the 40 μm pixels on account of their smaller size, the 10 μm pixel image lag could not be measured from the LED data due to lack of signal. For all devices, the mean image lag of the 40 μm non-OBF pixels did not change following proton irradiation, remaining near zero (<0.5%) for signal ~500 to 5000 e^-.

4 Conclusion

Three BSI CIS221-X devices have been irradiated up to twice the EoL non-ionizing radiation dose for the THESEUS mission. Assessment of electro-optical performance before and after proton irradiation has shown no significant degradation of readout noise or image lag, whereas the mean dark current and number of hot pixels increased. The cause of this increase has been attributed to proton-induced bulk silicon defects. A CIS221-X previously exposed to ionizing radiation has been additionally irradiated with protons. This device exhibited a greater rate of dark current degradation than the devices irradiated with protons only. Further work is necessary to verify the repeatability of this result. Across all devices, the degradation in CIS221-X performance following proton irradiation is similar to that of comparable CMOS image sensors. This validates the consideration of the CIS221-X pixel design for the THESEUS SXI detectors. However, it is advised that the final flight model THESEUS SXI image sensors be retested under representative THESEUS in-orbit conditions.

Disclosures

There are no conflicts of interest to declare.

Code and Data Availability

The data that support the findings of this article are not publicly available. They can be requested from the author at charles.townsend-rose@open.ac.uk

Acknowledgments

This program is funded by ESA under the E/0901-01 Technology Development Element "CMOS Image Sensor for X-ray Applications."

References

1. L. Amati et al., "The THESEUS space mission concept: science case, design and expected performances," *Adv. Space Res.* **62**, 191–244 (2018).
2. L. Amati et al., "The THESEUS space mission: updated design, profile and expected performances," *Proc. SPIE* **11444**, 114442J (2021).
3. THESEUS Team, *THESEUS Assessment Study Report (Yellow Book)*, ESA (2021).
4. M. W. J. Hubbard et al., "Impact of particle passage and focusing from micro-pore optics for radiation damage estimates," *J. Astron. Telesc. Instrum. Syst.* **10**(3), 034003 (2024).
5. J. Heymes et al., "Development of a photon-counting near-Fano-limited x-ray CMOS image sensor for THESEUS' SXI," *Proc. SPIE* **11454**, 114540I (2020).
6. K. D. Stefanov et al., "Design and performance of a pinned photodiode CMOS image sensor using reverse substrate bias," *Sensors* **18**(1), 118 (2018).
7. C. Townsend-Rose et al., "Electro-optical characterization of a CMOS image sensor optimized for soft x-ray astronomy," *J. Astron. Telesc. Instrum. Syst.* **9**(4), 046001 (2023).
8. C. Townsend-Rose et al., "Ionising radiation effects in a soft X-ray CMOS image sensor," *Nucl. Instrum. Method. Phys. Res. Sect. A* **1059**, 169011 (2024).
9. C. Townsend-Rose et al., "Non-ionising radiation effects in a soft x-ray CMOS image sensor," *Proc. SPIE* **13103**, 131031B (2024).
10. ESCC, *Guidelines for Displacement Damage Irradiation Testing* (2021).
11. M. R. Soman et al., "Proton irradiation of the CIS115 for the JUICE mission," *Proc. SPIE* **9602**, 96020O (2015).
12. M. Liu et al., "Radiation effects on scientific CMOS sensors for X-ray astronomy: I. Proton irradiation," *J. Astron. Telesc. Instrum. Syst.* **9**(4), 046003 (2023).
13. ASIF, "Fluence to TID dose converter for protons and ions," 2023, http://www.asif.asi.it/ (accessed 22 January 2024).
14. ASIF, "Fluence to TNID dose converter for protons and ions," 2023, http://www.asif.asi.it/ (accessed 22 January 2024).
15. D. Parker and C. Wheldon, "The Birmingham MC40 cyclotron facility," *Nucl. Phys. News* **28**(4), 15–20 (2018).
16. K. D. Stefanov et al., "A CMOS image sensor for soft X-ray astronomy," *Proc. SPIE* **12191**, 121910N (2022).

Biographies of the authors are not available.